Published for SISSA by Springer

Received: March 21, 2013
Accepted: June 7, 2013
Published: June 28, 2013

Search for CP violation in $D^+ \to \phi\pi^+$ and $D_s^+ \to K_S^0\pi^+$ decays

The LHCb collaboration

E-mail: hamish.gordon@cern.ch

Abstract: A search for CP violation in $D^+ \to \phi\pi^+$ decays is performed using data collected in 2011 by the LHCb experiment corresponding to an integrated luminosity of $1.0\,\text{fb}^{-1}$ at a centre of mass energy of 7 TeV. The CP-violating asymmetry is measured to be $(-0.04 \pm 0.14 \pm 0.14)\%$ for candidates with K^-K^+ mass within $20\,\text{MeV}/c^2$ of the ϕ meson mass. A search for a CP-violating asymmetry that varies across the ϕ mass region of the $D^+ \to K^-K^+\pi^+$ Dalitz plot is also performed, and no evidence for CP violation is found. In addition, the CP asymmetry in the $D_s^+ \to K_S^0\pi^+$ decay is measured to be $(0.61 \pm 0.83 \pm 0.14)\%$.

Keywords: CP violation, Charm physics, Hadron-Hadron Scattering

ArXiv ePrint: 1303.4906

doi:10.1007/JHEP06(2013)112

JHEP06(2013)112

Contents

JHEP06(2013)112

1 Introduction

Cabibbo-suppressed charm decays are the focus of searches for direct *CP* violation (CPV) in the charm sector. In these decays, direct CPV will occur if tree and loop (penguin) processes interfere with different strong and weak phases. Furthermore, contributions from physics beyond the Standard Model may appear in the virtual loops [1]. Evidence for direct CPV in charm decays was reported by LHCb and subsequently by CDF using the $D^0 \to K^-K^+$ and $D^0 \to \pi^-\pi^+$ channels [2, 3]. Although the latest results do not confirm the evidence for CPV in the charm sector [4, 5], further studies using different decay modes remain well motivated. The large branching ratios of $D^0 \to K^-K^+$ compared to $D^0 \to \pi^-\pi^+$ decays, and of the $D^+ \to K^-K^+\pi^+$ compared to the $D^+ \to \pi^-\pi^+\pi^+$ mode, suggest that the contribution of the penguin amplitude may be significant in both $D^0 \to K^-K^+$ and $D^+ \to K^-K^+\pi^+$ decays [6]. The inclusion of charge conjugate decays is implied where appropriate throughout this paper. In D^+ decays, a non-zero *CP* asymmetry would indicate unambiguously the presence of direct CPV. The $D^+ \to \phi\pi^+$ decay is a particularly promising channel for CPV searches due to its large branching ratio of $(2.65 \pm 0.09) \times 10^{-3}$ [7]. A recent investigation of this decay at the Belle experiment yielded a *CP*-violating charge asymmetry of $(+0.51 \pm 0.28 \pm 0.05)\%$ [8], while BaBar measured $(-0.3 \pm 0.3 \pm 0.5)\%$ [9].

Searches for CPV in charm decays with the LHCb experiment rely on a good understanding of the charge asymmetries both in D meson production in pp collisions and in the detection of the final states. These effects are studied using control decay modes in which no CPV is expected, and cancelled by measuring the differences in asymmetries between different final states or by comparing measurements made in one area of the Dalitz plot relative to another.

To investigate CPV in the $D^+ \to \phi\pi^+$ decay, the $D^+ \to K^0_S\pi^+$ decay with $K^0_S \to \pi^-\pi^+$ is used as a control channel. This decay is itself sensitive to CPV via the interference of Cabibbo-favoured and doubly Cabibbo-suppressed amplitudes. However, the *CP* asymmetry in this channel is predicted to be at most 0.01% in the Standard Model [10], and there is less scope for contributions from non-Standard Model dynamics than in the $D^+ \to \phi\pi^+$ decay as no penguin amplitudes contribute [1]. Therefore CPV in the $D^+ \to K^0_S\pi^+$ decay is assumed to be negligible. The *CP* asymmetry in the $D^+ \to \phi\pi^+$ region of the $D^+ \to K^-K^+\pi^+$ Dalitz plot is given by, to first order,

$$A_{\rm CP}(D^+ \to \phi\pi^+) = A_{\rm raw}(D^+ \to \phi\pi^+) - A_{\rm raw}(D^+ \to K^0_S\pi^+) + A_{\rm CP}(K^0/\overline{K}^0), \qquad (1.1)$$

where the raw charge asymmetry $A_{\rm raw}$ is defined as

$$A_{\rm raw} = \frac{N_{D^+} - N_{D^-}}{N_{D^+} + N_{D^-}}, \qquad (1.2)$$

for yields $N_{D^\pm}$ of positively- or negatively-charged signal or control-mode candidates. The kaon asymmetry $A_{\rm CP}(K^0/\overline{K}^0)$ is the correction for CPV in the neutral kaon system and is -0.028% with a systematic uncertainty of 0.028% [11]. To first order, the use of the control channel cancels the effects of the $D^\pm$ production asymmetry of $(-0.96 \pm 0.26 \pm 0.18)\%$ [11] and of any asymmetry associated with the detection of the pion [12]. In the proximity of the ϕ meson mass of $1019.46 \pm 0.02\,{\rm MeV}/c^2$ [7] in the $D^+ \to K^-K^+\pi^+$ Dalitz plot, the kaons have almost identical momentum distributions. Therefore the kaon interaction asymmetry cancels between the K^+ and K^- meson daughters of the ϕ resonance. Hence the search is restricted to decays with K^+K^- invariant masses in the range $1.00 < m_{K^-K^+} < 1.04\,{\rm GeV}/c^2$.

A concurrent measurement of the *CP* asymmetry in the $D^+_s \to K^0_S\pi^+$ decay, approximated as

$$A_{\rm CP}(D^+_s \to K^0_S\pi^+) = A_{\rm raw}(D^+_s \to K^0_S\pi^+) - A_{\rm raw}(D^+_s \to \phi\pi^+) + A_{\rm CP}(K^0/\overline{K}^0), \qquad (1.3)$$

is performed using the $D^+_s \to \phi\pi^+$ decay as a control channel. This decay is also Cabibbo-suppressed, with similar contributions from loop amplitudes as the $D^+ \to \phi\pi^+$ decay, but the number of signal candidates is substantially lower. This is partly due to the lower D^+_s production cross-section [13] and partly because only K^0_S mesons with decay times of less than 40 ps are used in this analysis. In eq. (1.3), the effect of the CPV in the neutral kaon system has a sign opposite to that in eq. (1.1) relative to the raw asymmetry in the $D^+_{(s)} \to K^0_S\pi^+$ decay because the D^+_s decays predominantly to a K^0 meson while the D^+ decays to a $\overline{K}^0$.

Within the Standard Model, CPV in singly Cabibbo-suppressed charm decays with contributing tree and penguin amplitudes is expected to be [15]

$$A_{\rm CP} \approx \left| Im\left(\frac{V_{ub}V^*_{cb}}{V_{us}V^*_{cs}}\right)\right| R \sin\delta_S, \qquad (1.4)$$

where R is a number of order one that depends on hadronic matrix elements, δ_S is the strong phase difference between tree and penguin amplitudes, and V_{ij} are elements of the CKM

JHEP06(2013)112

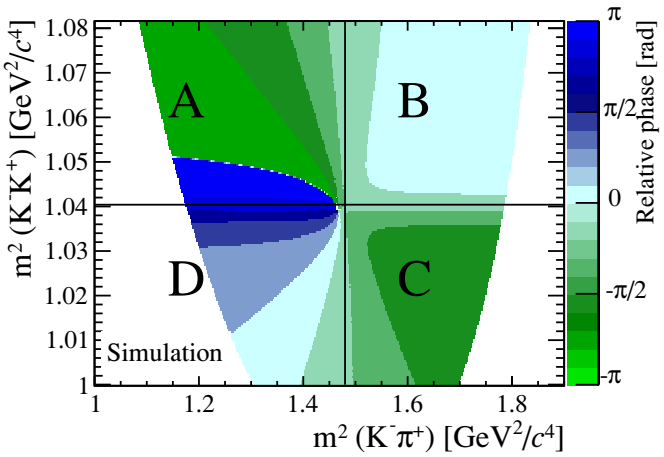

Figure 1. Variation of the overall phase of the D^+ decay amplitude in the ϕ mass region of the Dalitz plot, from a simulation study based on the CLEO-c amplitude model in which the phase is defined relative to that of the $K^*(892)^0$ resonance [14]. To calculate $A_{\rm CP}|_S$, the region is divided into rectangular zones as shown, corresponding to $1.00 < m(K^-K^+) < 1.02\,\text{GeV}/c^2$ and $1.02 < m(K^-K^+) < 1.04\,\text{GeV}/c^2$ along the y-axis, and to $m^2(K^-\pi^+) < 1.48\,\text{GeV}^2/c^4$ and $m^2(K^-\pi^+) > 1.48\,\text{GeV}^2/c^4$ along the x-axis.

matrix. In the region of the ϕ resonance in the $D^+ \to K^-K^+\pi^+$ Dalitz plot, several other amplitudes contribute to the overall matrix element and interfere with the ϕ meson [9, 14]. A recent amplitude analysis of this decay mode from the CLEO-c collaboration [14] yields a matrix element with a relative strong phase that varies rapidly across the ϕ region, as shown in figure 1. The isobar amplitude model favoured by CLEO-c (fit 'B' in ref. [14]) contains major contributions from the ϕ, $K^*(892)^0$, $K_0^*(1430)^0$ and $K_0^*(800)$ resonances. The phase is measured relative to that of the $K^*(892)^0$ meson. The variation in phase means that it is possible that a constant *CP*-violating asymmetry could be cancelled out when the different regions of the ϕ resonance are combined to calculate $A_{\rm CP}$. Hence we define a complementary observable called $A_{\rm CP}|_S$. The area around the ϕ resonance in the Dalitz plot is split into four rectangular regions $A - D$ defined clockwise from the top-left as shown in figure 1. The division is chosen to minimise the change in phase within each region. A difference between the two diagonals, each made of two regions with similar phases, is calculated as

$$A_{\rm CP}|_S = \frac{1}{2}\left(A^A_{\rm raw} + A^C_{\rm raw} - A^B_{\rm raw} - A^D_{\rm raw}\right). \tag{1.5}$$

This observable is not affected by the $D^\pm$ production asymmetry and is robust against systematic biases from the detector.

To test the hypothesis that $A_{\rm CP}|_S$ can sometimes be more sensitive to *CP* violation than $A_{\rm CP}$, a study is performed using simulated pseudo-experiments in which plausible types of CPV are introduced into the CLEO-c amplitude model [14]. The matrix elements for D^+ and D^- decays are separately modified in a number of ways, as specified in table 1, and events are generated from the resulting probability density functions. In each simulated sample, approximately the same number of events as in the dataset are produced, and the

JHEP06(2013)112

Type of CPV	Mean A_{CP} (%)	Mean $A_{CP}\|_S$ (%)
3° in ϕ phase	-0.01 (0.1σ)	-1.02 (5.1σ)
0.8% in ϕ amplitude	-0.50 (2.5σ)	-0.02 (0.1σ)
4° in $K_0^*(1430)^0$ phase	0.52 (2.6σ)	-0.89 (4.5σ)
4° in $K_0^*(800)$ phase	0.70 (3.5σ)	0.10 (0.5σ)

Table 1. Expected mean values of A_{CP} and $A_{CP}|_S$ for different types of *CP* violation introduced into the simulated Dalitz plots, together with the significance with which a signal could be observed given estimated overall uncertainties in A_{CP} and $A_{CP}|_S$ of 0.2%.

values of A_{CP} and $A_{CP}|_S$ are compared. The effects of background and of the reconstruction and signal selection efficiency variation across the ϕ region are negligible.

The level of CPV in the pseudo-experiments is chosen to give an expected result with significance of around three Gaussian standard deviations in at least one observable. For each type of CPV, twenty Dalitz plots are simulated. The mean values of A_{CP} and $A_{CP}|_S$ in these pseudo-experiments are given in table 1, together with the significance with which these signals could be observed in the dataset under study. The table indicates that some types of CPV can be observed more effectively with A_{CP} and others with $A_{CP}|_S$.

It was found in ref. [16] that the sensitivity to CPV can vary substantially with the details of the amplitude model. Therefore these simple simulations should not be treated as accurate predictions, but instead as a guide to the relative sensitivity of the two observables.

2 Detector

The LHCb detector [17] is a single-arm forward spectrometer covering the pseudorapidity range $2 < \eta < 5$, designed for the study of particles containing b or c quarks. The detector includes a high precision tracking system consisting of a silicon-strip vertex detector (VELO) surrounding the pp interaction region, a large-area silicon-strip detector located upstream of a dipole magnet with a bending power of about 4 Tm, and three stations of silicon-strip detectors and straw drift tubes placed downstream. The combined tracking system has momentum resolution $\Delta p/p$ that varies from 0.4% at 5 GeV/c to 0.6% at 100 GeV/c, and impact parameter resolution of 20 µm for tracks with high transverse momentum p_T. Charged hadrons are identified using two ring-imaging Cherenkov detectors. Photon, electron and hadron candidates are identified by a calorimeter system consisting of scintillating-pad and preshower detectors, an electromagnetic calorimeter and a hadronic calorimeter. Muons are identified by a system composed of alternating layers of iron and multiwire proportional chambers. The trigger [18] consists of a hardware stage, based on information from the calorimeter and muon systems, an inclusive software stage, which uses the tracking system, and a second software stage that exploits the full event information.

3 Dataset and selection

The data sample used in this analysis corresponds to an integrated luminosity of 1.0 fb^{-1} of pp collisions at a centre of mass energy of 7 TeV, and was collected by the LHCb experiment

JHEP06(2013)112

in 2011. The polarity of the LHCb magnet was changed several times during the run, and approximately half of the data were taken with each polarity, referred to as 'magnet-up' and 'magnet-down' data hereafter. To optimise the event selection and estimate background contributions, 12.5 million pp collision events containing $D^+ \to K^0_S\pi^+$, $K^0_S \to \pi^-\pi^+$ decays and 5 million events containing $D^+ \to K^-K^+\pi^+$ decays are simulated with Pythia 6.4 [19] with a specific LHCb configuration [20]. Hadron decays are described by EvtGen [21]. The interaction of the generated particles with the detector and its response are implemented using the Geant4 toolkit [22, 23] as described in ref. [24].

To ensure the dataset is unbiased, the trigger must accept candidates in well-defined ways that can be shown to be charge-symmetric. A trigger decision may be based on part or all of the $D^+_{(s)}$ signal candidate, on other particles in the event, or both. For example, signal decays triggered at the hardware level exclusively by the pion from the $D^+_{(s)}$ decay are not used, as they are shown in section 5 to have large detector-dependent charge asymmetries. For an event to be accepted by the hardware trigger, two criteria, not mutually exclusive, are used: the decision must be based on one of the daughter tracks of the K^0_S or ϕ meson, or on a particle other than the decay products of the $D^+_{(s)}$ candidate. In the first case the same track must also activate the inclusive software trigger. This software trigger requires that one of the tracks from the signal $D^+_{(s)}$ candidate has $p_T > 1.7\,\text{GeV}/c$ and distance of closest approach to the primary vertex (PV) of at least 0.1 mm. The second stage of the software trigger is required to find combinations of three tracks that meet the criteria to be signal decays.

Candidate $D^+_{(s)} \to \phi\pi^+$ decays are reconstructed by combining the tracks from two oppositely charged particles that are identified by the RICH detectors as kaons with one track identified as a pion. The combined invariant mass of the two kaons is required to lie in the range $1.00 < m_{K^-K^+} < 1.04\,\text{GeV}/c^2$. The scalar sum of the p_T of the daughter particles must exceed $2.8\,\text{GeV}/c$.

To reconstruct $D^+_{(s)} \to K^0_S\pi^+$ candidates, pairs of oppositely charged particles with a pion mass hypothesis are combined to form K^0_S candidates. Only those with $p_T > 700\,\text{MeV}/c$ and invariant mass within $35\,\text{MeV}/c^2$ of the world average K^0_S mass [7] are retained. Accepted candidates are then combined with a third charged particle, the bachelor pion, to form a $D^+_{(s)}$ candidate. The mass of the K^0_S meson is constrained to its known value in the kinematic fit. All three pion tracks must be detected in the VELO, so only K^0_S mesons with short decay times are used.

Further requirements are applied in order to reduce background from random track combinations and partially reconstructed charm and B decays. Both K^0_S and $D^+_{(s)}$ candidates are required to have a vertex with acceptable fit quality. Daughters of the ϕ and K^0_S mesons must have momentum $p > 2\,\text{GeV}/c$ and $p_T > 250\,\text{MeV}/c$. Impact parameter requirements are used to ensure that all the daughters of the $D^+_{(s)}$ candidate do not originate at any PV in the event. To remove non-resonant $D^+ \to \pi^-\pi^+\pi^+$ candidates, the K^0_S meson decay vertex must be displaced by at least 10 mm in the forward direction from the decay vertex of its parent D^+ meson. The bachelor pion in both final states must have $p > 5\,\text{GeV}/c$ and $p_T > 500\,\text{MeV}/c$, must not come from any PV, and must be positively identified as a pion rather than as a kaon, electron or muon. In addition, fiducial

JHEP06(2013)112

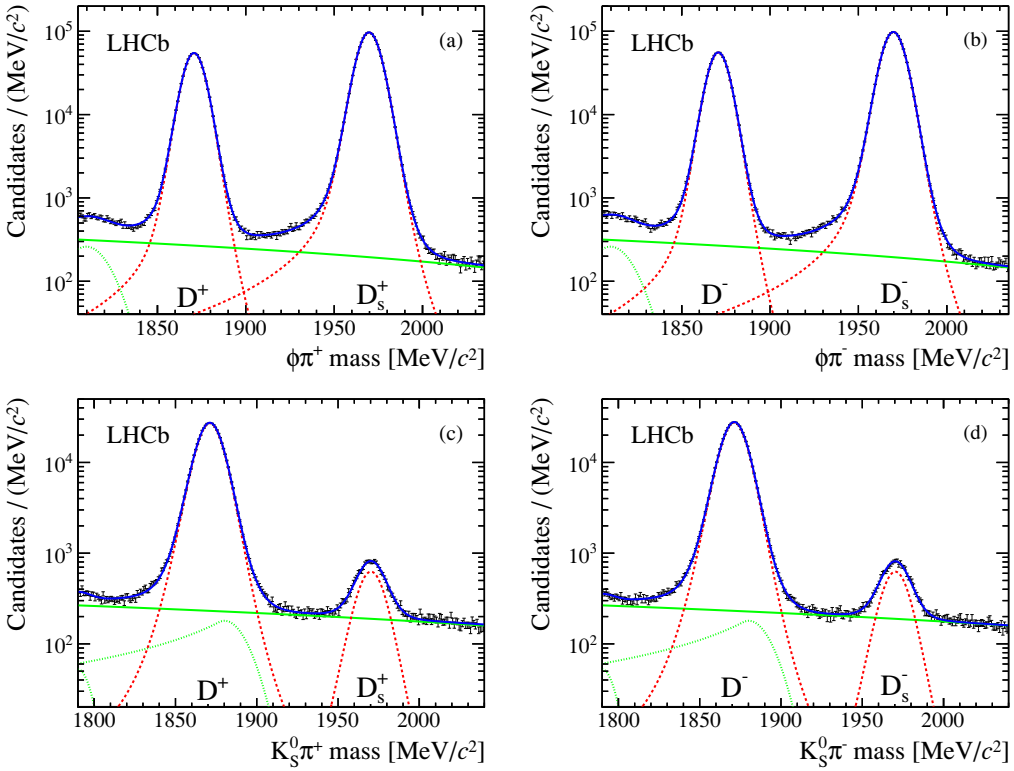

Figure 2. Invariant mass distribution of selected (a) $D^+ \to \phi\pi^+$, (b) $D^- \to \phi\pi^-$, (c) $D^+ \to K^0_S\pi^+$ and (d) $D^- \to K^0_S\pi^-$ candidates. The data are represented by symbols with error bars. The red dashed curves indicate the signal lineshapes, the green solid lines represent the combinatorial background shape, and the green dotted lines represent background from mis-reconstructed $D^+_s \to \phi\pi^+\pi^0$ decays in (a) and (b), and $D^+_s \to K^0_S\pi^+\pi^0$ or $D^+_s \to K^0_S K^+$ decays in (c) and (d). The blue solid lines show the sum of all fit components.

requirements are applied [2] to exclude regions with a large tracking efficiency asymmetry. The $D^+_{(s)}$ candidate is required to have $1.5 < p_{\rm T} < 20.0\,{\rm GeV}/c$ and pseudorapidity η in the range $2.2 < \eta < 4.4$, to point to a PV (to suppress D from B decays), and to have a decay time significantly greater than zero. The proportion of events with more than one $D^+_{(s)}$ candidate is negligible.

The invariant mass distributions of selected candidates in the two final states are presented in figure 2. After applying the selection and trigger requirements, 1,203,930 $D^\pm_{(s)} \to K^0_S\pi^\pm$ and 4,704,810 $D^\pm_{(s)} \to \phi\pi^\pm$ candidates remain in the mass ranges shown in the figure. The distribution of decays in the ϕ region of the $D^+ \to K^-K^+\pi^+$ Dalitz plot is shown in figure 3.

4 Determination of the yields and asymmetries

For the measurement of $A_{\rm CP}$, the signal yields are measured in 12 bins of transverse momentum $p_{\rm T}$ and pseudorapidity η, using binned likelihood fits to the distributions of the invariant masses m, where m is either $m_{\phi\pi^+}$ or $m_{K^0_S\pi^+}$. The values of $A_{\rm CP}$ in each bin

JHEP06(2013)112

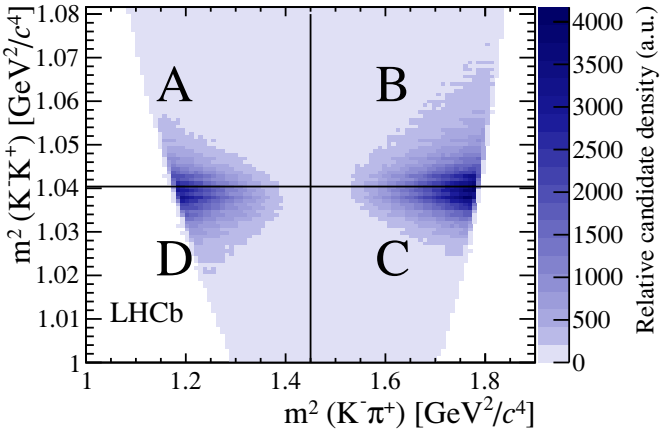

Figure 3. Observed density of decays in the $D^+ \to K^-K^+\pi^+$ Dalitz plot, with the regions A-D labelled as described in the text.

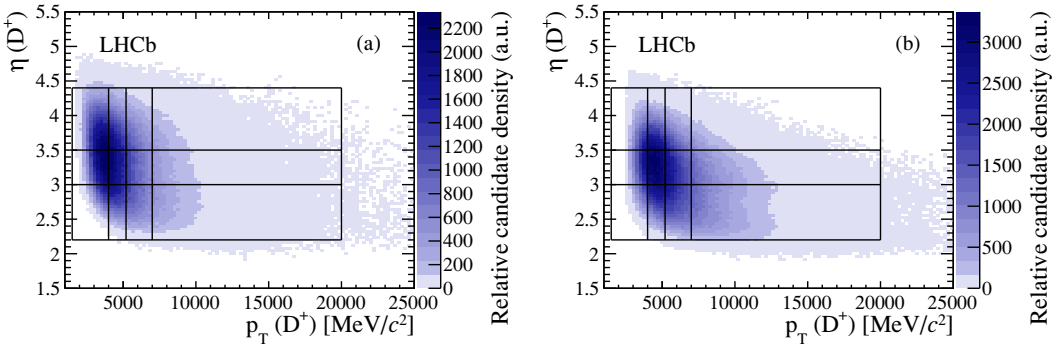

Figure 4. Distributions of transverse momentum $p_{\rm T}$ and pseudorapidity η for (a) $D^+ \to K^0_{\rm S}\pi^+$ and (b) $D^+ \to \phi\pi^+$ candidates with invariant masses m in the range $1845 < m < 1895\,{\rm MeV}/c^2$. Candidates that do not fall into the 12 rectangular bins are not used in the analysis.

are calculated and a weighted average over the bins is performed to obtain the final result. This procedure is adopted because the distributions of the two decays in $p_{\rm T}$ and η differ slightly, as shown in figure 4, and the $D^\pm$ production asymmetry may also vary over this range [11]. The $p_{\rm T} - \eta$ binning therefore reduces a potential source of systematic bias. The shapes of the $D^+_{(s)} \to K^0_{\rm S}\pi^+$ mass peaks are described by single Cruijff functions [25],

$$f(m) \propto \exp\left[\frac{-(m-\mu)^2}{2\sigma^2 + (m-\mu)^2\alpha_{L,R}}\right] \tag{4.1}$$

with the peak position defined by the free parameter μ, the width by σ, and the tails by α_L and α_R. The parameter α_L is used for $m < \mu$ and α_R for $m > \mu$. In the $\phi\pi^+$ final state, Crystal Ball functions [26] are added to the Cruijff functions to account for the tails of the mass peaks. The signal lineshapes are tested on simulated data and found to describe the data well. The background is fitted with a straight line and an additional Gaussian component centred at low mass to account for partially reconstructed $D_s^+ \to K^0_{\rm S}(\phi)\pi^+\pi^0$ decays. This background mostly lies outside the interval in invariant mass that is fitted.

JHEP06(2013)112

Decay mode	Signal yield ($\times 10^3$)
$D^+ \to \phi\pi^+$	1576.9 ± 1.5
$D_s^+ \to \phi\pi^+$	3010.2 ± 2.2
$D^+ \to K_S^0\pi^+$	1057.8 ± 1.2
$D_s^+ \to K_S^0\pi^+$	25.6 ± 0.2

Table 2. Numbers of signal candidates in the four decay modes from the mass fits, with statistical uncertainties only.

In the $K_S^0\pi^+$ case there is also a cross-feed component from the $D_s^+ \to K_S^0K^+$ decay mode, where the K^+ meson is misidentified as a pion. In the fit to data, the cross-feed yield and charge asymmetry are allowed to vary but the shape is fixed from the simulation. It is modelled by a Crystal Ball function. The yield of cross-feed is found to be small, at 6014 ± 817 decays, or 0.57% of the D^+ yield.

The fits are performed simultaneously over four subsamples ($D_{(s)}^+$ magnet-up, $D_{(s)}^+$ magnet-down, $D_{(s)}^-$ magnet-up, and $D_{(s)}^-$ magnet-down data) with the peak positions, widths and yields of the $D_{(s)}^+$ and background allowed to vary independently in the four subsamples. All other parameters are shared. The peak positions are found to differ between charges and magnet polarities by around $0.2\,\mathrm{MeV}/c^2$. The raw asymmetries are then determined from the yields. The fitted yields are given in in table 2.

The results are cross-checked with a sideband subtraction procedure under the assumption of a linear background. The background is sufficiently small relative to the signal in the $D^+ \to \phi\pi^+$ channel that the charge asymmetry can be calculated by counting D^+ and D^- candidates in a mass interval defined around the D^+ mass of $1845 < m < 1895\,\mathrm{MeV}/c^2$. Therefore, the yields for $A_{\mathrm{CP}}|_S$ are evaluated using this simple technique. The resolution in the Dalitz plot is improved by constraining the D^+ candidate mass to the world average value [7], instead of leaving it as a free parameter. This has a small effect which is assigned as a systematic uncertainty in section 5. In the measurement of A_{CP}, the background in the $D^+ \to K_S^0\pi^+$ channel is larger and therefore the results are taken from fits.

5 Systematic uncertainties and cross-checks

The analysis methods are constructed to ensure that systematic biases on the raw charge asymmetries cancel in the end result. The dominant systematic uncertainties in both A_{CP} and $A_{\mathrm{CP}}|_S$ are determined by considering control decay channels in which no asymmetry is expected.

The main systematic uncertainty in A_{CP} results from kinematic differences between the $\phi\pi^+$ and $K_S^0\pi^+$ final states, which lead to imperfections in the cancellation of detector asymmetries between them. Some detector asymmetries arise from small differences in the tracking efficiency or acceptance across the bending plane of the magnet, i.e. between the left and right halves of the detector. The response of the hardware trigger is also known to be asymmetric, because it does not take into account which way particles bend

JHEP06(2013)112

in the magnetic field when it measures their transverse energy $E_{\rm T}$ or $p_{\rm T}$. In data taken with one magnet polarity, a pion from a D^+ decay will bend in the opposite direction to a pion from a D^- decay, and if one of these pions is bent into an inefficient part of the tracking system and is lost while the other is detected, a charge asymmetry will result. The same situation could occur if one pion is bent inwards and so does not meet the hadron trigger $E_{\rm T}$ threshold while a pion of the opposite charge is bent outwards and therefore has enough measured $E_{\rm T}$ to activate the trigger. This cancels to a good approximation between the left and right halves of the detector, but any left/right asymmetry in the calorimeters or muon stations could result in imperfect cancellation, biasing the charge asymmetry. The effect of these asymmetries on this analysis is not eliminated by the subtraction of the asymmetries in the two final states in eq. 1.1 as the two decays do not have identical kinematic properties. Thus, in the data taken with one magnet polarity, the charge asymmetry can be affected. However, when the magnet polarity is reversed, the bias on the asymmetry changes sign because the particles are deflected in the opposite directions. The values of $A_{\rm CP}$ in $D^+ \to \phi\pi^+$ decays are found to differ by $(0.81 \pm 0.28)\%$ between the data taken with magnet polarity up and data taken with polarity down. The effect is removed, to a very good approximation, by combining results obtained with opposite magnet polarities, $A_{\rm CP}^{\uparrow}$ and $A_{\rm CP}^{\downarrow}$, in an average with equal weights,

$$A_{\rm CP} = \frac{A_{\rm CP}^{\uparrow} + A_{\rm CP}^{\downarrow}}{2}. \tag{5.1}$$

However, non-cancelling effects can bias the measurement and are considered as sources of systematic uncertainty. The data triggered by the $K_{\rm S}^0$ or ϕ meson at the hardware level are charge-symmetric to a good approximation, and are assumed to be unbiased. However, in data triggered by another particle in the event, the particle that activates the trigger may be correlated to the signal decay. For example, a signal decay is often accompanied by a $D^{\pm}$ meson of the opposite charge. If this meson decays to a charged hadron, electron or muon, the daughter particle, which is more likely to have the opposite charge to the signal $D^{\pm}$, could fire the trigger. The different kinematics and acceptance of the signal and control channel studied in this analysis mean that the cancellation of charge-asymmetric trigger efficiencies between them may not be complete. To study the size of this effect, a sample of approximately 57 million $D^+ \to K^-\pi^+\pi^+$ decays is selected using the same criteria as those for the signal. The charge asymmetries in the differently triggered datasets are given in table 3. Small but significant discrepancies between data from different triggers are observed, indicating that the hardware triggers may introduce small biases into the dataset. The large difference between magnet up and magnet down data in the sample that is triggered by the muon detectors is due to a charge-asymmetric $p_{\rm T}$ threshold in the detector, but this cancels when the magnet polarities are averaged. A systematic uncertainty equal to the maximum deviation from the average charge asymmetry of $(-2.034 \pm 0.014)\%$ in any of the triggers is assigned. This occurs in the electron trigger and the difference is 0.114%. The precision with which effects cancel between $\phi\pi^+$ and $K_{\rm S}^0\pi^+$ final states in the analysis cannot be quantified accurately. Therefore the most conservative approach is adopted and no cancellation is assumed.

JHEP06(2013)112

Trigger type	Magnet up	Magnet down	Average	Difference
Hadron	-2.037 ± 0.032	-1.970 ± 0.027	-2.003 ± 0.021	-0.068 ± 0.042
Muon	-2.361 ± 0.041	-1.607 ± 0.035	-1.984 ± 0.027	-0.754 ± 0.053
Electron	-2.094 ± 0.048	-2.201 ± 0.041	-2.148 ± 0.031	0.106 ± 0.063
Photon	-1.937 ± 0.070	-2.230 ± 0.060	-2.083 ± 0.046	0.293 ± 0.092
Overall average	-2.128 ± 0.021	-1.940 ± 0.018	-2.034 ± 0.014	-0.188 ± 0.028

Table 3. Raw charge asymmetries, in %, in samples of the $D^+ \to K^-\pi^+\pi^+$ control decay in which a particle not from the signal decay activated various hardware triggers.

Binning	Change in $A_{\rm CP}$ ($\times 10^{-4}$)
No binning	8.3 ± 3.7
12 bins ($3 \times D^+_{(s)}$ $p_{\rm T}$, $4 \times D^+_{(s)}$ η)	0.6 ± 1.7
48 bins ($8 \times D^+_{(s)}$ $p_{\rm T}$, $6 \times D^+_{(s)}$ η)	-2.9 ± 1.1
192 bins ($2 \times \pi^+$ p, $8 \times \pi^+$ ϕ, $4 \times D^+_{(s)}$ $p_{\rm T}$, $3 \times D^+_{(s)}$ η)	-2.4 ± 1.1
180 bins ($3 \times \pi^+$ $p_{\rm T}$, $5 \times \pi^+$ η, $4 \times D^+_{(s)}$ $p_{\rm T}$, $3 \times D^+_{(s)}$ η)	3.5 ± 2.6
1440 bins ($3 \times \pi^+$ $p_{\rm T}$, $5 \times \pi^+$ η, $8 \times \pi^+$ ϕ, $4 \times D^+_{(s)}$ $p_{\rm T}$, $3 \times D^+_{(s)}$ η)	2.5 ± 1.6

Table 4. Changes to the final result observed with various alternative kinematic binning schemes. The default scheme uses four bins of $D^+_{(s)}$ $p_{\rm T}$ and three bins of $D^+_{(s)}$ η. The variable ϕ is the azimuthal angle around the proton beams. The statistical uncertainties are determined by subtracting the uncertainties on the alternative result and the default result in quadrature.

Residual detector asymmetry differences between the $D^+ \to \phi\pi^+$ and $D^+ \to K^0_{\rm S}\pi^+$ decays due to their different kinematics are studied by applying several different kinematic binning schemes to the data. The measured asymmetry is found to be stable with variations in the binning, suggesting that the detector asymmetries are small. The results are summarised in table 4. The largest discrepancy in raw asymmetry, as expected, results from using no kinematic binning, as this does not account for any variation of the $D^\pm$ production asymmetry across the kinematic region. The next largest difference with respect to the baseline binning scheme, of 0.035%, is assigned as a systematic uncertainty on the asymmetry due to residual kinematic differences between decay modes.

The $A_{\rm CP}|_S$ observable is highly robust against systematic uncertainties. Any effect that does not vary across the Dalitz plot will cancel in the subtraction in eq. 1.5, and effects that do vary with $K^-\pi^+$ or K^-K^+ invariant mass across the ϕ region will also cancel when the regions are combined in the diagonal difference. For example, the asymmetry in the interaction of the charged kaons with the detector material would affect the asymmetry difference between decays with high and low values of $K^-\pi^+$ invariant mass, which is correlated with the momenta of the kaons. However such effects cancel to a good approximation in both observables, as shown below. Only quantities that vary between the diagonals of the Dalitz plot region would lead to significant systematic biases on $A_{\rm CP}|_S$. To test for the presence of such effects, $A_{\rm CP}|_S$ is calculated in the $D^+_s \to \phi\pi^+$ control decay,

JHEP06(2013)112

which has similar kinematics to the signal despite the different Dalitz plot distributions of the events. The result is $(-0.120 \pm 0.119)\%$, which is compatible with zero as expected. The statistical uncertainty on this result, added in quadrature to the central value, gives a measure of the precision with which detector effects are known to cancel. Thus a value of 0.169% is assigned as the main systematic uncertainty in $A_{\rm CP}|_S$.

The systematic uncertainty due to charged kaon interaction asymmetries is studied by determining the effect on the result of enlarging the size of the K^-K^+ mass window under study. This increases the differences between the momentum spectra of the kaons, which increases the effect of the interaction asymmetry because it depends strongly on momentum. The consistency of this procedure is checked with simulation studies. The systematic uncertainty is found to be 0.031% in $A_{\rm CP}$ for the D^+ decay, 0.002% for $A_{\rm CP}$ in the D_s^+ decay and 0.009% in $A_{\rm CP}|_S$.

The asymmetric interaction of the neutral kaons with detector material is studied using the method outlined in ref. [27] to account for coherent regeneration. The amount of material each kaon passes through before it decays and the predicted differences between the K^0 and $\overline{K}^0$ material interaction cross sections [28] are used to determine an expected asymmetry. The size of the effect is found to be $(0.039 \pm 0.004)\%$, where the uncertainty is due to imperfect knowledge of the amount of material in the detector. This is consistent with the dependence of the asymmetry on the depth of material passed through by the kaons seen in data. The asymmetry is assigned as a systematic uncertainty on the $A_{\rm CP}$ measurements.

A systematic uncertainty of 0.056% is associated with the resolution in the Dalitz plot variables for $A_{\rm CP}|_S$, due to candidates migrating across the boundaries of the regions $A - D$. This is determined by taking the difference between results before and after the D^+ mass is constrained to the world average value. This procedure is repeated for $A_{\rm CP}$, but as expected the systematic uncertainty is much smaller.

Further small systematic uncertainties arise from the mass fitting, from the calculation of the effect of the CPV in the neutral kaon system [11], from the choice of fiducial cuts, from modelling of the cross-feed in the $D^+ \to K^0_{\rm S}\pi^+$ decay, and from neglecting the background in the calculation of $A_{\rm CP}|_S$. In the simulation, the contribution of D from B decays is found to differ between the final states by around 1%, and this leads to another small uncertainty since the production asymmetries for B and D decays may differ.

Other potential sources of systematic uncertainty, such as the difference in selection criteria between the two final states, are negligible. The kinematic distributions of daughter particles are checked for biases. The variation of the asymmetries with time during the data taking period is also considered. The systematic uncertainties are summarised in table 5.

As a further cross check, the difference in raw asymmetry between the $D_s^+ \to \phi\pi^+$ and $D_s^+ \to \pi^-\pi^+\pi^+$ decays is calculated. Since these are both Cabibbo-favoured tree-level decays, this quantity is expected to be zero. The $D_s^+ \to \pi^-\pi^+\pi^+$ decay has reasonably similar kinematic properties and a similar yield in our dataset to the $D^+ \to K^0_{\rm S}\pi^+$ decay, and the $D_s^+ \to \phi\pi^+$ is very similar to the corresponding D^+ decay. Thus the kinematic differences between the final states in the D_s^+ control decays are similar to those in the D^+ signal channels.

JHEP06(2013)112

Source	$A_{\rm CP}$ (D^+) [%]	$A_{\rm CP}$ (D_s^+) [%]	$A_{\rm CP}\vert_S$ [%]
Triggers	0.114	0.114	n/a
D_s^+ control sample size	n/a	n/a	0.169
Kaon asymmetry	0.031	0.002	0.009
Binning	0.035	0.035	n/a
Resolution	0.007	0.006	0.056
Regeneration	0.039	0.039	n/a
Fitting	0.033	0.033	n/a
Kaon *CP* violation	0.028	0.028	n/a
Fiducial effects	0.022	0.022	n/a
Backgrounds	0.008	n/a	0.007
D from B	0.003	0.015	0.003
Total	0.138	0.136	0.178

Table 5. Systematic uncertainties on the three measurements. The abbreviation n/a is used where the systematic effect does not apply. The row labelled 'Backgrounds' represents the uncertainty in modelling the cross-feed in $A_{\rm CP}$ and the uncertainty from ignoring the background in $A_{\rm CP}\vert_S$.

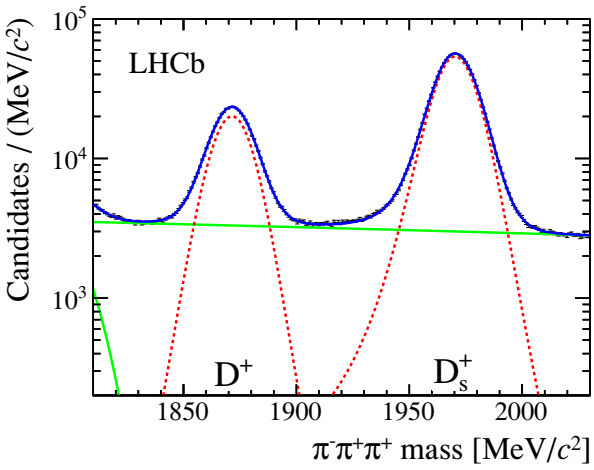

Figure 5. Invariant mass distribution of selected $D^{\pm}_{(s)} \to \pi^{\mp}\pi^{\pm}\pi^{\pm}$ decays. The data are represented by symbols with error bars. The red dashed peaks indicate the signal decays, the green solid lines represent the combinatorial background shape, and the green dotted lines represent backgrounds from mis-reconstructed $D_s^+ \to \pi^-\pi^+\pi^+\pi^0$ decays. The blue solid line shows the sum of all fit components.

The $D_s^+ \to \pi^-\pi^+\pi^+$ decay is reconstructed using the same selection as for the signal decays. The hardware trigger must be activated by a particle that does not form part of the signal decay, or by the π^- meson, or by a random π^+ meson. The resulting sample has a large background due to random pions from the primary vertex. To remove this, the regions of the $D_s^+ \to \pi^-\pi^+\pi^+$ Dalitz plot in which one of the pions has a low momentum in the

JHEP06(2013)112

D_s^+ rest frame are excluded from the sample by removing the areas of the Dalitz plot below the $f_0(980)$ resonance. The requirement on $\pi^-\pi^+$ invariant mass $m^2_{\pi^-\pi^+} > 0.75\,\mathrm{GeV}^2/c^4$ is applied to both $\pi^-\pi^+$ meson pairs. The mass distribution of the candidates that remain is fitted with a Cruijff function in the 12 kinematic bins described in section 4 and the raw charge asymmetries in the D_s^+ decay are calculated.

The weighted average of the raw asymmetry differences in the 12 kinematic bins is $(0.22 \pm 0.12)\%$. The systematic uncertainty on this is similar to that on the main analysis, or 0.13%, so the result differs from zero by 1.3 standard deviations. This discrepancy is assumed to be a statistical fluctuation and no additional uncertainty is assigned.

Many additional cross-checks and comparisons of the data samples are performed. The raw asymmetries are consistent with those observed in the measurements of the D^+ and D_s^+ production asymmetries [11, 12]. The different triggers used in the analysis give statistically compatible results. A study of the values of A_{CP} in individual bins gives no indication of any dependence on p_{T} and η. The regions $A - D$ used in the calculation of $A_{\mathrm{CP}}|_S$ have fully compatible asymmetries.

6 Results and conclusion

Searches for *CP* violation in the ϕ region of the $D^+ \to K^-K^+\pi^+$ Dalitz plot and in the $D_s^+ \to K^0_{\mathrm{S}}\pi^+$ decay mode are performed. The results are

$$\begin{aligned} A_{\mathrm{CP}}(D^+ \to \phi\pi^+) &= (-0.04 \pm 0.14 \pm 0.14)\%, \\ A_{\mathrm{CP}}|_S(D^+ \to \phi\pi^+) &= (-0.18 \pm 0.17 \pm 0.18)\%, \\ A_{\mathrm{CP}}(D_s^+ \to K^0_{\mathrm{S}}\pi^+) &= (+0.61 \pm 0.83 \pm 0.14)\%, \end{aligned}$$

consistent with existing measurements. The first and third measurements assume negligible *CP* violation effects in the $D^+ \to K^0_{\mathrm{S}}\pi^+$ and $D_s^+ \to \phi\pi^+$ control channels, respectively. The $A_{\mathrm{CP}}|_S$ observable is shown to increase the sensitivity of the analysis to certain types of *CP* violation significantly, but there is no evidence for *CP* violation in either decay. This is the most precise analysis of *CP* violation in the ϕ region of the $D^+ \to K^-K^+\pi^+$ Dalitz plot to date. The results suggest that any CP asymmetries in decays within this region are unlikely to exceed the approximate level of effects currently believed to be possible within the Standard Model.

Acknowledgments

We express our gratitude to our colleagues in the CERN accelerator departments for the excellent performance of the LHC. We thank the technical and administrative staff at the LHCb institutes. We acknowledge support from CERN and from the national agencies: CAPES, CNPq, FAPERJ and FINEP (Brazil); NSFC (China); CNRS/IN2P3 and Region Auvergne (France); BMBF, DFG, HGF and MPG (Germany); SFI (Ireland); INFN (Italy); FOM and NWO (The Netherlands); SCSR (Poland); ANCS/IFA (Romania); MinES,

JHEP06(2013)112

Rosatom, RFBR and NRC "Kurchatov Institute" (Russia); MinECo, XuntaGal and GENCAT (Spain); SNSF and SER (Switzerland); NAS Ukraine (Ukraine); STFC (United Kingdom); NSF (USA). We also acknowledge the support received from the ERC under FP7. The Tier1 computing centres are supported by IN2P3 (France), KIT and BMBF (Germany), INFN (Italy), NWO and SURF (The Netherlands), PIC (Spain), GridPP (United Kingdom). We are thankful for the computing resources put at our disposal by Yandex LLC (Russia), as well as to the communities behind the multiple open source software packages that we depend on.

JHEP06(2013)112

References

[1] Y. Grossman, A.L. Kagan and Y. Nir, *New physics and CP-violation in singly Cabibbo suppressed D decays*, *Phys. Rev.* **D 75** (2007) 036008 [hep-ph/0609178] [INSPIRE].

[2] LHCb collaboration, *Evidence for CP-violation in time-integrated $D^0 \to h^-h^+$ decay rates*, *Phys. Rev. Lett.* **108** (2012) 111602 [arXiv:1112.0938] [INSPIRE].

[3] CDF collaboration, T. Aaltonen et al., *Measurement of the difference of CP-violating asymmetries in $D^0 \to K^+K^-$ and $D^0 \to \pi^+\pi^-$ decays at CDF*, *Phys. Rev. Lett.* **109** (2012) 111801 [arXiv:1207.2158] [INSPIRE].

[4] LHCb collaboration, *Search for direct CP violation in $D^0 \to h^-h^+$ modes using semileptonic B decays*, *Phys. Lett.* **B 723** (2013) 33 [arXiv:1303.2614] [INSPIRE].

[5] LHCb collaboration, *A search for time-integrated CP-violation in $D^0 \to K^-K^+$ and $D^0 \to \pi^-\pi^+$ decays*, LHCb-CONF-2013-003 (2013).

[6] J. Brod, Y. Grossman, A.L. Kagan and J. Zupan, *A consistent picture for large penguins in $D \to \pi^+\pi^-, K^+K^-$*, *JHEP* **10** (2012) 161 [arXiv:1203.6659] [INSPIRE].

[7] Particle Data Group collaboration, J. Beringer et al., *Review of particle physics*, *Phys. Rev.* **D 86** (2012) 010001 [INSPIRE].

[8] Belle collaboration, M. Staric et al., *Search for CP-violation in $D^\pm$ meson decays to $\phi\pi^\pm$*, *Phys. Rev. Lett.* **108** (2012) 071801 [arXiv:1110.0694] [INSPIRE].

[9] BaBar collaboration, J. Lees et al., *Search for direct CP-violation in singly-Cabibbo suppressed $D^\pm \to K^+K^-\pi^\pm$ decays*, *Phys. Rev.* **D 87** (2013) 052010 [arXiv:1212.1856] [INSPIRE].

[10] I.I. Bigi and H. Yamamoto, *Interference between Cabibbo allowed and doubly forbidden transitions in $D \to K_S, K_L + \pi$'s decays*, *Phys. Lett.* **B 349** (1995) 363 [hep-ph/9502238] [INSPIRE].

[11] LHCb collaboration, *Measurement of the $D^\pm$ production asymmetry in 7 TeV pp collisions*, *Phys. Lett.* **B 718** (2013) 902 [arXiv:1210.4112] [INSPIRE].

[12] LHCb collaboration, *Measurement of the D_s^+-D_s^- production asymmetry in 7 TeV pp collisions*, *Phys. Lett.* **B 713** (2012) 186 [arXiv:1205.0897] [INSPIRE].

[13] LHCb collaboration, *Prompt charm production in pp collisions at* $\sqrt{s} = 7$ *TeV*, *Nucl. Phys.* **B 871** (2013) 1 [arXiv:1302.2864] [INSPIRE].

[14] CLEO collaboration, P. Rubin et al., *Search for CP-violation in the Dalitz-plot analysis of* $D^{\pm} \to K^+K^-\pi^{\pm}$, *Phys. Rev.* **D 78** (2008) 072003 [arXiv:0807.4545] [INSPIRE].

[15] D. Atwood and A. Soni, *Searching for the origin of CP-violation in Cabibbo suppressed D-meson decays*, arXiv:1211.1026 [INSPIRE].

[16] LHCb collaboration, *Search for CP-violation in* $D^+ \to K^-K^+\pi^+$ *decays*, *Phys. Rev.* **D 84** (2011) 112008 [arXiv:1110.3970] [INSPIRE].

[17] LHCb collaboration, *The LHCb Detector at the LHC*, 2008 *JINST* **3** S08005 [INSPIRE].

[18] R. Aaij et al., *The LHCb trigger and its performance in 2011*, 2013 *JINST* **8** P04022 [arXiv:1211.3055] [INSPIRE].

[19] T. Sjöstrand, S. Mrenna and P.Z. Skands, *PYTHIA 6.4 physics and manual*, *JHEP* **05** (2006) 026 [hep-ph/0603175] [INSPIRE].

[20] I. Belyaev et al., *Handling of the generation of primary events in* GAUSS*, the LHCb simulation framework*, *IEEE Nucl. Sci. Symp. Conf. Rec.* (2010) 1155.

[21] D. Lange, *The EvtGen particle decay simulation package*, *Nucl. Instrum. Meth.* **A 462** (2001) 152 [INSPIRE].

[22] GEANT4 collaboration, J. Allison et al., *Geant4 developments and applications*, *IEEE Trans. Nucl. Sci.* **53** (2006) 270.

[23] GEANT4 collaboration, S. Agostinelli et al., *GEANT4: a simulation toolkit*, *Nucl. Instrum. Meth.* **A 506** (2003) 250 [INSPIRE].

[24] M. Clemencic et al., *The LHCb simulation application,* GAUSS*: design, evolution and experience*, J. Phys. Conf. Ser **331** (2011) 032023.

[25] BABAR collaboration, P. del Amo Sanchez et al., *Study of* $B \to X\gamma$ *decays and determination of* $|V_{td}/V_{ts}|$, *Phys. Rev.* **D 82** (2010) 051101 [arXiv:1005.4087] [INSPIRE].

[26] T. Skwarnicki, *A study of the radiative cascade transitions between the* Υ' *and* Υ *resonances*, Ph.D. thesis, Institute of Nuclear Physics, Krakow, Poland (1986) [INSPIRE].

[27] B. Ko, E. Won, B. Golob and P. Pakhlov, *Effect of nuclear interactions of neutral kaons on CP asymmetry measurements*, *Phys. Rev.* **D 84** (2011) 111501 [arXiv:1006.1938] [INSPIRE].

[28] A. Gsponer et al., *Precise coherent* K_S *regeneration amplitudes for C, Al, Cu, Sn and Pb nuclei from 20-GeV/c to 140-GeV/c and their interpretation*, *Phys. Rev. Lett.* **42** (1979) 13 [INSPIRE].

JHEP06(2013)112

The LHCb collaboration

R. Aaij[40], C. Abellan Beteta[35,n], B. Adeva[36], M. Adinolfi[45], C. Adrover[6], A. Affolder[51], Z. Ajaltouni[5], J. Albrecht[9], F. Alessio[37], M. Alexander[50], S. Ali[40], G. Alkhazov[29], P. Alvarez Cartelle[36], A.A. Alves Jr[24,37], S. Amato[2], S. Amerio[21], Y. Amhis[7], L. Anderlini[17,f], J. Anderson[39], R. Andreassen[59], R.B. Appleby[53], O. Aquines Gutierrez[10], F. Archilli[18], A. Artamonov [34], M. Artuso[56], E. Aslanides[6], G. Auriemma[24,m], S. Bachmann[11], J.J. Back[47], C. Baesso[57], V. Balagura[30], W. Baldini[16], R.J. Barlow[53], C. Barschel[37], S. Barsuk[7], W. Barter[46], Th. Bauer[40], A. Bay[38], J. Beddow[50], F. Bedeschi[22], I. Bediaga[1], S. Belogurov[30], K. Belous[34], I. Belyaev[30], E. Ben-Haim[8], M. Benayoun[8], G. Bencivenni[18], S. Benson[49], J. Benton[45], A. Berezhnoy[31], R. Bernet[39], M.-O. Bettler[46], M. van Beuzekom[40], A. Bien[11], S. Bifani[12], T. Bird[53], A. Bizzeti[17,h], P.M. Bjørnstad[53], T. Blake[37], F. Blanc[38], J. Blouw[11], S. Blusk[56], V. Bocci[24], A. Bondar[33], N. Bondar[29], W. Bonivento[15], S. Borghi[53], A. Borgia[56], T.J.V. Bowcock[51], E. Bowen[39], C. Bozzi[16], T. Brambach[9], J. van den Brand[41], J. Bressieux[38], D. Brett[53], M. Britsch[10], T. Britton[56], N.H. Brook[45], H. Brown[51], I. Burducea[28], A. Bursche[39], G. Busetto[21,q], J. Buytaert[37], S. Cadeddu[15], O. Callot[7], M. Calvi[20,j], M. Calvo Gomez[35,n], A. Camboni[35], P. Campana[18,37], A. Carbone[14,c], G. Carboni[23,k], R. Cardinale[19,i], A. Cardini[15], H. Carranza-Mejia[49], L. Carson[52], K. Carvalho Akiba[2], G. Casse[51], M. Cattaneo[37], Ch. Cauet[9], M. Charles[54], Ph. Charpentier[37], P. Chen[3,38], N. Chiapolini[39], M. Chrzaszcz [25], K. Ciba[37], X. Cid Vidal[36], G. Ciezarek[52], P.E.L. Clarke[49], M. Clemencic[37], H.V. Cliff[46], J. Closier[37], C. Coca[28], V. Coco[40], J. Cogan[6], E. Cogneras[5], P. Collins[37], A. Comerma-Montells[35], A. Contu[15], A. Cook[45], M. Coombes[45], S. Coquereau[8], G. Corti[37], B. Couturier[37], G.A. Cowan[38], D. Craik[47], S. Cunliffe[52], R. Currie[49], C. D'Ambrosio[37], P. David[8], P.N.Y. David[40], I. De Bonis[4], K. De Bruyn[40], S. De Capua[53], M. De Cian[39], J.M. De Miranda[1], M. De Oyanguren Campos[35,o], L. De Paula[2], W. De Silva[59], P. De Simone[18], D. Decamp[4], M. Deckenhoff[9], L. Del Buono[8], D. Derkach[14], O. Deschamps[5], F. Dettori[41], A. Di Canto[11], H. Dijkstra[37], M. Dogaru[28], S. Donleavy[51], F. Dordei[11], A. Dosil Suárez[36], D. Dossett[47], A. Dovbnya[42], F. Dupertuis[38], R. Dzhelyadin[34], A. Dziurda[25], A. Dzyuba[29], S. Easo[48,37], U. Egede[52], V. Egorychev[30], S. Eidelman[33], D. van Eijk[40], S. Eisenhardt[49], U. Eitschberger[9], R. Ekelhof[9], L. Eklund[50], I. El Rifai[5], Ch. Elsasser[39], D. Elsby[44], A. Falabella[14,e], C. Färber[11], G. Fardell[49], C. Farinelli[40], S. Farry[12], V. Fave[38], D. Ferguson[49], V. Fernandez Albor[36], F. Ferreira Rodrigues[1], M. Ferro-Luzzi[37], S. Filippov[32], C. Fitzpatrick[37], M. Fontana[10], F. Fontanelli[19,i], R. Forty[37], O. Francisco[2], M. Frank[37], C. Frei[37], M. Frosini[17,f], S. Furcas[20], E. Furfaro[23], A. Gallas Torreira[36], D. Galli[14,c], M. Gandelman[2], P. Gandini[54], Y. Gao[3], J. Garofoli[56], P. Garosi[53], J. Garra Tico[46], L. Garrido[35], C. Gaspar[37], R. Gauld[54], E. Gersabeck[11], M. Gersabeck[53], T. Gershon[47,37], Ph. Ghez[4], V. Gibson[46], V.V. Gligorov[37], C. Göbel[57], D. Golubkov[30], A. Golutvin[52,30,37], A. Gomes[2], H. Gordon[54], M. Grabalosa Gándara[5], R. Graciani Diaz[35], L.A. Granado Cardoso[37], E. Graugés[35], G. Graziani[17], A. Grecu[28], E. Greening[54], S. Gregson[46], O. Grünberg[58], B. Gui[56], E. Gushchin[32], Yu. Guz[34], T. Gys[37], C. Hadjivasiliou[56], G. Haefeli[38], C. Haen[37], S.C. Haines[46], S. Hall[52], T. Hampson[45], S. Hansmann-Menzemer[11], N. Harnew[54], S.T. Harnew[45], J. Harrison[53], T. Hartmann[58], J. He[7], V. Heijne[40], K. Hennessy[51], P. Henrard[5], J.A. Hernando Morata[36], E. van Herwijnen[37], E. Hicks[51], D. Hill[54], M. Hoballah[5], C. Hombach[53], P. Hopchev[4], W. Hulsbergen[40], P. Hunt[54], T. Huse[51], N. Hussain[54], D. Hutchcroft[51], D. Hynds[50], V. Iakovenko[43], M. Idzik[26], P. Ilten[12], R. Jacobsson[37], A. Jaeger[11], E. Jans[40], P. Jaton[38], F. Jing[3], M. John[54], D. Johnson[54], C.R. Jones[46], B. Jost[37], M. Kaballo[9], S. Kandybei[42], M. Karacson[37], T.M. Karbach[37], I.R. Kenyon[44], U. Kerzel[37], T. Ketel[41], A. Keune[38], B. Khanji[20], O. Kochebina[7], I. Komarov[38,31], R.F. Koopman[41], P. Koppenburg[40], M. Korolev[31], A. Kozlinskiy[40], L. Kravchuk[32], K. Kreplin[11],

JHEP06(2013)112

M. Kreps[47], G. Krocker[11], P. Krokovny[33], F. Kruse[9], M. Kucharczyk[20,25,j], V. Kudryavtsev[33], T. Kvaratskheliya[30,37], V.N. La Thi[38], D. Lacarrere[37], G. Lafferty[53], A. Lai[15], D. Lambert[49], R.W. Lambert[41], E. Lanciotti[37], G. Lanfranchi[18,37], C. Langenbruch[37], T. Latham[47], C. Lazzeroni[44], R. Le Gac[6], J. van Leerdam[40], J.-P. Lees[4], R. Lefèvre[5], A. Leflat[31,37], J. Lefrançois[7], S. Leo[22], O. Leroy[6], B. Leverington[11], Y. Li[3], L. Li Gioi[5], M. Liles[51], R. Lindner[37], C. Linn[11], B. Liu[3], G. Liu[37], J. von Loeben[20], S. Lohn[37], J.H. Lopes[2], E. Lopez Asamar[35], N. Lopez-March[38], H. Lu[3], D. Lucchesi[21,q], J. Luisier[38], H. Luo[49], F. Machefert[7], I.V. Machikhiliyan[4,30], F. Maciuc[28], O. Maev[29,37], S. Malde[54], G. Manca[15,d], G. Mancinelli[6], U. Marconi[14], R. Märki[38], J. Marks[11], G. Martellotti[24], A. Martens[8], L. Martin[54], A. Martín Sánchez[7], M. Martinelli[40], D. Martinez Santos[41], D. Martins Tostes[2], A. Massafferri[1], R. Matev[37], Z. Mathe[37], C. Matteuzzi[20], E. Maurice[6], A. Mazurov[16,32,37,e], J. McCarthy[44], R. McNulty[12], A. Mcnab[53], B. Meadows[59,54], F. Meier[9], M. Meissner[11], M. Merk[40], D.A. Milanes[8], M.-N. Minard[4], J. Molina Rodriguez[57], S. Monteil[5], D. Moran[53], P. Morawski[25], M.J. Morello[22,s], R. Mountain[56], I. Mous[40], F. Muheim[49], K. Müller[39], R. Muresan[28], B. Muryn[26], B. Muster[38], P. Naik[45], T. Nakada[38], R. Nandakumar[48], I. Nasteva[1], M. Needham[49], N. Neufeld[37], A.D. Nguyen[38], T.D. Nguyen[38], C. Nguyen-Mau[38,p], M. Nicol[7], V. Niess[5], R. Niet[9], N. Nikitin[31], T. Nikodem[11], A. Nomerotski[54], A. Novoselov[34], A. Oblakowska-Mucha[26], V. Obraztsov[34], S. Oggero[40], S. Ogilvy[50], O. Okhrimenko[43], R. Oldeman[15,d,37], M. Orlandea[28], J.M. Otalora Goicochea[2], P. Owen[52], B.K. Pal[56], A. Palano[13,b], M. Palutan[18], J. Panman[37], A. Papanestis[48], M. Pappagallo[50], C. Parkes[53], C.J. Parkinson[52], G. Passaleva[17], G.D. Patel[51], M. Patel[52], G.N. Patrick[48], C. Patrignani[19,i], C. Pavel-Nicorescu[28], A. Pazos Alvarez[36], A. Pellegrino[40], G. Penso[24,l], M. Pepe Altarelli[37], S. Perazzini[14,c], D.L. Perego[20,j], E. Perez Trigo[36], A. Pérez-Calero Yzquierdo[35], P. Perret[5], M. Perrin-Terrin[6], G. Pessina[20], K. Petridis[52], A. Petrolini[19,i], A. Phan[56], E. Picatoste Olloqui[35], B. Pietrzyk[4], T. Pilař[47], D. Pinci[24], S. Playfer[49], M. Plo Casasus[36], F. Polci[8], G. Polok[25], A. Poluektov[47,33], E. Polycarpo[2], D. Popov[10], B. Popovici[28], C. Potterat[35], A. Powell[54], J. Prisciandaro[38], V. Pugatch[43], A. Puig Navarro[38], G. Punzi[22,r], W. Qian[4], J.H. Rademacker[45], B. Rakotomiaramanana[38], M.S. Rangel[2], I. Raniuk[42], N. Rauschmayr[37], G. Raven[41], S. Redford[54], M.M. Reid[47], A.C. dos Reis[1], S. Ricciardi[48], A. Richards[52], K. Rinnert[51], V. Rives Molina[35], D.A. Roa Romero[5], P. Robbe[7], E. Rodrigues[53], P. Rodriguez Perez[36], S. Roiser[37], V. Romanovsky[34], A. Romero Vidal[36], J. Rouvinet[38], T. Ruf[37], F. Ruffini[22], H. Ruiz[35], P. Ruiz Valls[35,o], G. Sabatino[24,k], J.J. Saborido Silva[36], N. Sagidova[29], P. Sail[50], B. Saitta[15,d], C. Salzmann[39], B. Sanmartin Sedes[36], M. Sannino[19,i], R. Santacesaria[24], C. Santamarina Rios[36], E. Santovetti[23,k], M. Sapunov[6], A. Sarti[18,l], C. Satriano[24,m], A. Satta[23], M. Savrie[16,e], D. Savrina[30,31], P. Schaack[52], M. Schiller[41], H. Schindler[37], M. Schlupp[9], M. Schmelling[10], B. Schmidt[37], O. Schneider[38], A. Schopper[37], M.-H. Schune[7], R. Schwemmer[37], B. Sciascia[18], A. Sciubba[24], M. Seco[36], A. Semennikov[30], K. Senderowska[26], I. Sepp[52], N. Serra[39], J. Serrano[6], P. Seyfert[11], M. Shapkin[34], I. Shapoval[42,37], P. Shatalov[30], Y. Shcheglov[29], T. Shears[51,37], L. Shekhtman[33], O. Shevchenko[42], V. Shevchenko[30], A. Shires[52], R. Silva Coutinho[47], T. Skwarnicki[56], N.A. Smith[51], E. Smith[54,48], M. Smith[53], M.D. Sokoloff[59], F.J.P. Soler[50], F. Soomro[18,37], D. Souza[45], B. Souza De Paula[2], B. Spaan[9], A. Sparkes[49], P. Spradlin[50], F. Stagni[37], S. Stahl[11], O. Steinkamp[39], S. Stoica[28], S. Stone[56], B. Storaci[39], M. Straticiuc[28], U. Straumann[39], V.K. Subbiah[37], S. Swientek[9], V. Syropoulos[41], M. Szczekowski[27], P. Szczypka[38,37], T. Szumlak[26], S. T'Jampens[4], M. Teklishyn[7], E. Teodorescu[28], F. Teubert[37], C. Thomas[54], E. Thomas[37], J. van Tilburg[11], V. Tisserand[4], M. Tobin[39], S. Tolk[41], D. Tonelli[37], S. Topp-Joergensen[54], N. Torr[54], E. Tournefier[4,52], S. Tourneur[38], M.T. Tran[38], M. Tresch[39], A. Tsaregorodtsev[6], P. Tsopelas[40], N. Tuning[40], M. Ubeda Garcia[37], A. Ukleja[27], D. Urner[53], U. Uwer[11], V. Vagnoni[14], G. Valenti[14],

JHEP06(2013)112

R. Vazquez Gomez[35], P. Vazquez Regueiro[36], S. Vecchi[16], J.J. Velthuis[45], M. Veltri[17,g], G. Veneziano[38], M. Vesterinen[37], B. Viaud[7], D. Vieira[2], X. Vilasis-Cardona[35,n], A. Vollhardt[39], D. Volyanskyy[10], D. Voong[45], A. Vorobyev[29], V. Vorobyev[33], C. Voß[58], H. Voss[10], R. Waldi[58], R. Wallace[12], S. Wandernoth[11], J. Wang[56], D.R. Ward[46], N.K. Watson[44], A.D. Webber[53], D. Websdale[52], M. Whitehead[47], J. Wicht[37], J. Wiechczynski[25], D. Wiedner[11], L. Wiggers[40], G. Wilkinson[54], M.P. Williams[47,48], M. Williams[55], F.F. Wilson[48], J. Wishahi[9], M. Witek[25], S.A. Wotton[46], S. Wright[46], S. Wu[3], K. Wyllie[37], Y. Xie[49,37], F. Xing[54], Z. Xing[56], Z. Yang[3], R. Young[49], X. Yuan[3], O. Yushchenko[34], M. Zangoli[14], M. Zavertyaev[10,a], F. Zhang[3], L. Zhang[56], W.C. Zhang[12], Y. Zhang[3], A. Zhelezov[11], A. Zhokhov[30], L. Zhong[3], A. Zvyagin[37]

[1] *Centro Brasileiro de Pesquisas Físicas (CBPF), Rio de Janeiro, Brazil*
[2] *Universidade Federal do Rio de Janeiro (UFRJ), Rio de Janeiro, Brazil*
[3] *Center for High Energy Physics, Tsinghua University, Beijing, China*
[4] *LAPP, Université de Savoie, CNRS/IN2P3, Annecy-Le-Vieux, France*
[5] *Clermont Université, Université Blaise Pascal, CNRS/IN2P3, LPC, Clermont-Ferrand, France*
[6] *CPPM, Aix-Marseille Université, CNRS/IN2P3, Marseille, France*
[7] *LAL, Université Paris-Sud, CNRS/IN2P3, Orsay, France*
[8] *LPNHE, Université Pierre et Marie Curie, Université Paris Diderot, CNRS/IN2P3, Paris, France*
[9] *Fakultät Physik, Technische Universität Dortmund, Dortmund, Germany*
[10] *Max-Planck-Institut für Kernphysik (MPIK), Heidelberg, Germany*
[11] *Physikalisches Institut, Ruprecht-Karls-Universität Heidelberg, Heidelberg, Germany*
[12] *School of Physics, University College Dublin, Dublin, Ireland*
[13] *Sezione INFN di Bari, Bari, Italy*
[14] *Sezione INFN di Bologna, Bologna, Italy*
[15] *Sezione INFN di Cagliari, Cagliari, Italy*
[16] *Sezione INFN di Ferrara, Ferrara, Italy*
[17] *Sezione INFN di Firenze, Firenze, Italy*
[18] *Laboratori Nazionali dell'INFN di Frascati, Frascati, Italy*
[19] *Sezione INFN di Genova, Genova, Italy*
[20] *Sezione INFN di Milano Bicocca, Milano, Italy*
[21] *Sezione INFN di Padova, Padova, Italy*
[22] *Sezione INFN di Pisa, Pisa, Italy*
[23] *Sezione INFN di Roma Tor Vergata, Roma, Italy*
[24] *Sezione INFN di Roma La Sapienza, Roma, Italy*
[25] *Henryk Niewodniczanski Institute of Nuclear Physics Polish Academy of Sciences, Kraków, Poland*
[26] *AGH University of Science and Technology, Kraków, Poland*
[27] *National Center for Nuclear Research (NCBJ), Warsaw, Poland*
[28] *Horia Hulubei National Institute of Physics and Nuclear Engineering, Bucharest-Magurele, Romania*
[29] *Petersburg Nuclear Physics Institute (PNPI), Gatchina, Russia*
[30] *Institute of Theoretical and Experimental Physics (ITEP), Moscow, Russia*
[31] *Institute of Nuclear Physics, Moscow State University (SINP MSU), Moscow, Russia*
[32] *Institute for Nuclear Research of the Russian Academy of Sciences (INR RAN), Moscow, Russia*
[33] *Budker Institute of Nuclear Physics (SB RAS) and Novosibirsk State University, Novosibirsk, Russia*
[34] *Institute for High Energy Physics (IHEP), Protvino, Russia*
[35] *Universitat de Barcelona, Barcelona, Spain*
[36] *Universidad de Santiago de Compostela, Santiago de Compostela, Spain*
[37] *European Organization for Nuclear Research (CERN), Geneva, Switzerland*
[38] *Ecole Polytechnique Fédérale de Lausanne (EPFL), Lausanne, Switzerland*
[39] *Physik-Institut, Universität Zürich, Zürich, Switzerland*
[40] *Nikhef National Institute for Subatomic Physics, Amsterdam, The Netherlands*

JHEP06(2013)112

[41] *Nikhef National Institute for Subatomic Physics and VU University Amsterdam, Amsterdam, The Netherlands*
[42] *NSC Kharkiv Institute of Physics and Technology (NSC KIPT), Kharkiv, Ukraine*
[43] *Institute for Nuclear Research of the National Academy of Sciences (KINR), Kyiv, Ukraine*
[44] *University of Birmingham, Birmingham, United Kingdom*
[45] *H.H. Wills Physics Laboratory, University of Bristol, Bristol, United Kingdom*
[46] *Cavendish Laboratory, University of Cambridge, Cambridge, United Kingdom*
[47] *Department of Physics, University of Warwick, Coventry, United Kingdom*
[48] *STFC Rutherford Appleton Laboratory, Didcot, United Kingdom*
[49] *School of Physics and Astronomy, University of Edinburgh, Edinburgh, United Kingdom*
[50] *School of Physics and Astronomy, University of Glasgow, Glasgow, United Kingdom*
[51] *Oliver Lodge Laboratory, University of Liverpool, Liverpool, United Kingdom*
[52] *Imperial College London, London, United Kingdom*
[53] *School of Physics and Astronomy, University of Manchester, Manchester, United Kingdom*
[54] *Department of Physics, University of Oxford, Oxford, United Kingdom*
[55] *Massachusetts Institute of Technology, Cambridge, MA, United States*
[56] *Syracuse University, Syracuse, NY, United States*
[57] *Pontifícia Universidade Católica do Rio de Janeiro (PUC-Rio), Rio de Janeiro, Brazil, associated to*[2]
[58] *Institut für Physik, Universität Rostock, Rostock, Germany, associated to*[11]
[59] *University of Cincinnati, Cincinnati, OH, United States, associated to*[56]

[a] *P.N. Lebedev Physical Institute, Russian Academy of Science (LPI RAS), Moscow, Russia*
[b] *Università di Bari, Bari, Italy*
[c] *Università di Bologna, Bologna, Italy*
[d] *Università di Cagliari, Cagliari, Italy*
[e] *Università di Ferrara, Ferrara, Italy*
[f] *Università di Firenze, Firenze, Italy*
[g] *Università di Urbino, Urbino, Italy*
[h] *Università di Modena e Reggio Emilia, Modena, Italy*
[i] *Università di Genova, Genova, Italy*
[j] *Università di Milano Bicocca, Milano, Italy*
[k] *Università di Roma Tor Vergata, Roma, Italy*
[l] *Università di Roma La Sapienza, Roma, Italy*
[m] *Università della Basilicata, Potenza, Italy*
[n] *LIFAELS, La Salle, Universitat Ramon Llull, Barcelona, Spain*
[o] *IFIC, Universitat de Valencia-CSIC, Valencia, Spain*
[p] *Hanoi University of Science, Hanoi, Viet Nam*
[q] *Università di Padova, Padova, Italy*
[r] *Università di Pisa, Pisa, Italy*
[s] *Scuola Normale Superiore, Pisa, Italy*

JHEP06(2013)112